Integral microalgae-bacteria model (BIO_ALGAE): application to wastewater high rate algal ponds

Alessandro Solimeno[a], Lauren Parker[b], Tryg Lundquist[b], Joan García[a,*]

[a]GEMMA – Group of Environmental Engineering and Microbiology, Department of Civil and Environmental Engineering, Universitat Politècnica de Catalunya-BarcelonaTech, c/Jordi Girona, 1-3, Building D1, E-08034, Barcelona, Spain.

[b]Civil and Environmental Engineering Department, California Polytechnic State University, San Luis Obispo, California, 93407

Abstract

Reactions and processes that occur in microalgae and bacteria systems are difficult to understand because most of them take place simultaneously and they are strongly interdependent. In comparison with conventional wastewater treatment technologies, less is known about the physical, chemical and biochemical reactions and processes that occur in microalgae-bacteria treatment systems, such as high rate algal ponds (HRAP). In this paper we develop an integral mechanistic model describing the complex interactions in mixed algal-bacterial systems. The model includes crucial physical, chemical and biokinetic processes of microalgae as well as bacteria in wastewater. Carbon-limited microalgae and autotrophic bacteria growth, light attenuation, photorespiration, temperature and pH dependency are some of the new features included. The model named BIO_ALGAE was built using the general formulation and structure of activated sludge models (ASM), and it was implemented in COMSOL Multiphysics^{TM} platform. Calibration and validation were conducted with high quality experimental data from triplicated pilot HRAPs receiving real wastewater. Calibration was conducted adjusting 6 parameters selected after a Morris's sensitivity analysis: microalgae and heterotrophic bacteria specific growth rate, decay of heterotrophic bacteria and the transfer of gases to the atmosphere. The model was able to simulate the dynamics of different components in the ponds and the relative proportion of microalgae and bacteria. Furthermore, the model was used to investigate the relative effect of the factors that affect microalgae growth and the through practical study case the effect of different influent organic matter concentration on total biomass production and the relative proportions of microalgae and bacteria. The proposed model could be an efficient tool for industry to predict the production of microalgae, as well as to design and optimize the operations in contaminants removal from wastewater using algal-bacterial interactions.

Keywords:

Microalgae-bacteria model, wastewater, high rate algal ponds (HRAP), biomass production, microalgae/bacteria proportion, light attenuation, Monod kinetics.

Highlights

- New integral mechanistic model for microalgae-bacteria wastewater treatment systems is developed.

- The model was implemented in COMSOL Multiphysics^{TM} platform, calibrated and validated using experimental data for two different periods.

- The model was able to accurately reproduce the dynamics of different components of the system.

- Usefulness of the model was demonstrated with practical study case.

1. Introduction

In the past decade, an increasing amount of research has been conducted on microalgae-bacterial systems for wastewater treatment. These efforts were initially stimulated by the interest in producing biofuel from microalgae (Park and Craggs, 2011; Milano et al., 2016), but, compared to conventional wastewater treatment technologies, the potential total cost savings, including in electrical power, are great enough to pursue this topic independently of biofuels production (Suganya et al., 2016).

The system is based on the interactions of microalgae and bacteria in wastewater exposed to light. Algae photosynthesize and produce the oxygen used by bacteria, reducing or eliminating the need for mechanical aeration (Tricolici et al., 2014, Sayeda et al., 2016). Assimilation of nutrients (i.e. nitrogen and phosphorus) by algae is a further form of treatment (Liang et al., 2013), and pathogen inactivation also occurs in these algal-bacterial systems (Abdel et al., 2012).

Algal-bacterial wastewater treatment was originally carried-out in unmixed ponds – shallow oxidation ponds and deeper facultative ponds (Oswald and Gotaas, 1957), with mixed raceway ponds (specifically named high rate algal ponds) being introduced at full scale for increased cultivation control and algal productivity (Oswald et al., 1957). Using the produced algae biomass for biofuel feedstock was suggested shortly thereafter Oswald and Golueke (1960). Various other reactor designs have been proposed such as transparent vessels (e.g. tubular photobioreactors) and attached growth systems (e.g., algal turf scrubbers, Christenson and Sims, 2012). However, these other types of reactors are not a full scale reality, and belong to a more experimental domain in the field of wastewater treatment. These more complex and costly designs in comparison to mixed raceway ponds will be less competitive with conventional electromechanical treatment technologies.

In comparison with conventional treatment technologies, less is known about the physical, chemical and biochemical reactions and processes that occur in microalgae-bacteria wastewater treatment systems. Most of these reactions and processes take place simultaneously and they are strongly interdependent (García et al., 2006. Also, they are dependent on ever-changing outdoor environmental conditions such as light intensity, temperature, and the flow and quality of the influent wastewater. In order to predict performance and optimize reactor design, it is necessary to have a deep pond wastewater treatment system ecological understanding.

Mathematical models offer an opportunity to study microalgae-bacteria interactions, can provide useful tools for design, and can control real-world parameters, which can all lead to increase bioreactor efficiency (Bitog et al., 2011). While much

research has been conducted on microalgae models over the years (e.g. Dropp, 1968; Bernard et al., 2009), only recently has research intensively began on the integration of microalgal growth on biological wastewater treatment (microalgae-bacteria models). The very first modeling in this area was pioneered by Buhr and Miller (1983), and it focused on the simultaneous growth of algae and bacteria in high-rate algae ponds (HRAPs). HRAPs, which are shallow, low-energy, and paddle-wheel mixed treatment ponds, are typical in advanced pond wastewater treatment systems. Since Buhr and Miller (1983), other more sophisticated models have been developed mostly based on parameters and processes similar to those defined by the River Water Quality Model 1 (RWQM1) of the International Water Association (Reichert et al., 2011). However, while RWQM1 includes expressions for growth of microalgae on N (ammonium and nitrate) and P (orthophosphate), it does not include expressions for essential C limitations (carbon dioxide and bicarbonate) which can occur in algae growing in wastewater systems (Gehring et al., 2010). In the model by Sah et al. (2011) algal growth was described as a function of either ammonium or nitrate, with preference for ammonium. Halfhide et al. (2015) developed a simplified algae-bacteria model to simulate ammonia removal from wastewater, assuming the irradiance as limiting factor for algae growth. Likewise, Steen et al. (2015) proposed a simplified version of the Activated Sludge Model no. 3 (ASM3) based on the biomass growth of ammonia oxidizing bacteria, nitrite oxidizing bacteria, and microalgae.

Most of these previous models use a relatively low number of parameters to describe the inherent complexity of algae cultures and/or focus on single processes within the system, neither of which considers that microalgae-bacterial technologies are systemic processes that involve multiple components (e.g. carbon, nitrogen, and dissolved oxygen (DO)). For example, widely accepted microalgae-bacteria models, such as RWQM1 and Sah et al., (2011) do not include carbon limitation on the growth of microalgae and autotrophic bacteria and any reference to the effects of high value dissolved oxygen in culture medium on microalgae activity.

In this paper we complete the microalgae model previously developed by the authors (Solimeno et al., 2015, 2017), including crucial physical, chemical and biokinetic processes of microalgae as well as bacteria in wastewater treatment systems. The model, which is called BIO_ALGAE was mainly built by coupling the model of the authors (Solimeno et al., 2015) with the ASM3 (Iacopozzi et al., 2007). These models were used as base model to represent the microalgae and bacteria activity, respectively. The new most relevant features of the model are: the inclusion of carbon limitation on the growth of microalgae and the growth of autotrophic bacteria. Also, this model includes factors to represent photosynthesis, photolimitation, light attenuation, photorespiration, temperature dependency and the implementation of hydrodynamics in the system.

Altogether the main purpose of this study was to develop, calibrate and validate the integral microalgae and bacteria model with high quality experimental data from triplicate raceway ponds located at the Delhi, California wastewater pond treatment plant. The implementation of BIO_ALGAE in the COMSOL Multiphysics^{TM} software

allowed to simulate the dynamics of different components in the ponds and the relative proportion of microalgae and bacteria. Also the model was used for to applications: 1) to analyse the relative effect of the factors that affect microalgae growth, and 2) a study case on the effect of influent concentration of organic matter on the relative proportions of microalgae and bacteria. Our idea is to create a basis for a highly accepted platform that will be extensively used for different research purposes. Also, in the future, we believe that this model could help the industry to design and operate efficient systems.

2. Model description

2.1 Conceptual model

In order to facilitate the comprehension of the model, Fig. 1 shows a general simplified schematic representation of the conceptual model describing the complexity of microalgal-bacterial interactions.

Photosynthetic processes are activated with light. While microalgae (X_{ALG}) grow, they fix inorganic carbon (S_{CO2} and S_{HCO3}), consume substrates (S_{NH4}, S_{NO3} and S_{PO4}) present in wastewater and supply oxygen (S_{O2}) required by heterotrophic bacteria (X_H) to oxidize organic matter. During bacterial organic matter oxidation, CO_2 is produced and it is available for photosynthesis and nitrification. Nitrification is a two-step process: first ammonium oxidizing bacteria (X_{AOB}) convert ammonia and ammonium to nitrite (S_{NO2}) and second nitrate oxidizing bacteria (X_{NOB}) finish the conversion of nitrite to nitrate (S_{NO3}) (Diehl et al., 2007).

As result of microalgal activity, hydroxide ion concentrations (S_{OH}) and pH increase. With increasing pH, bicarbonate-carbonate equilibrium is displaced, pushing carbon species towards the formation of carbonate (S_{CO3}), lead ammonia volatilization, and phosphorus precipitation (Nurdogan and Oswald, 1995; Serodes et al., 1991).

In darkness, both heterotrophic bacteria (X_H) and microalgae (X_{ALG}) have a net CO_2 release through oxidation of organic matter and endogenous respiration, respectively. With this release, concentrations of hydrogen ions increase and pH decreases, and the bicarbonate-carbonate equilibrium shifts and the carbonate turn into bicarbonate (S_{HCO3}). This bicarbonate can be used as a substrate again in the presence of light. Microalgae respiration and bacterial growth reduce the oxygen level within the water. When oxygen levels are low, nitrate can become the primary source of oxygen, and denitrification occurs. This process is performed under anoxic conditions by denitrifying bacteria that reduce nitrate (S_{NO3}) into nitrogen gas. In fact, denitrifying bacteria are considered the same heterotrophic bacteria (X_H) that under oxygen depletion circumstances can facultative use S_{NO3} instead of S_{O2}.

Microalgae and bacteria processes are influenced by temperature, which also affects chemical equilibria, pH and gas solubility (Bouterfas et al., 2002). Furthermore, in HRAPs the excess of DO and CO_2 is gradually transferred from the culture medium to the atmosphere.

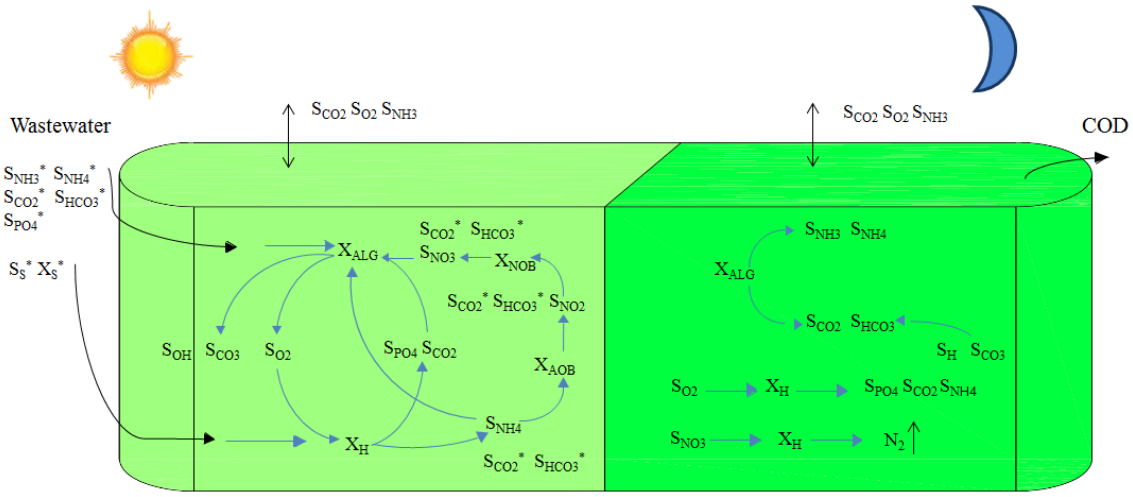

Fig. 1. General simplified schematic representation of the conceptual integrated model showing the main algal-bacterial interactions in a high rate algal pond, during day (left) and night (right). Components which enter the ponds with the influent are marked with * and processes are indicated by arrows. Particulate and dissolved components and processes are described in Sections 2.2.

2.2. Model components

The model uses the common nomenclature of the IWA models and considers 19 components – 6 particulate and 13 dissolved – implicated as variables in the physical, chemical and biokinetic processes. In the following two sections components are described, as well as their main role in processes and their interactions with other components.

2.2.1. Particulate components

In the model all particulate constituents (microorganisms as well as organic matter) are subject to decay except X_I (inert particulate organic matter). Microorganisms, of course, are subject to growth. None of these particulate organic constituents can be practically/easily distinguished from one another in the mixture of material in HRAPs. Microorganism concentrations listed below therefore can be modeled, but their experimental measurement is complicated. In fact, one tremendous advantage of the model is its capacity for predicting microorganisms concentrations.

1. **X_{ALG}** [g COD m^{-3}]: *Microalgae biomass*. It increases with growth processes pertinent to microalgae and decreases by endogenous respiration and inactivation of microalgae. Not present in influent wastewater.
2. **X_H** [g COD m^{-3}]: *Heterotrophic bacteria*. These organisms use organic matter as a source of carbon and energy. They growth in aerobic as well as anoxic heterotrophic conditions and decrease by endogenous respiration and decay. These bacteria are responsible for hydrolysis processes and they are also present in the wastewater influent.

3. **X_{AOB}** [g COD m^{-3}]: *Ammonium oxidizing bacteria*. Bacteria responsible for the first step of nitrification, the conversion of ammonium to nitrite. These microorganisms are produced by aerobic growth and decrease by endogenous respiration and decay. They are assumed to be present in the wastewater influent.
4. **X_{NOB}** [g COD m^{-3}]: *Nitrate oxidizing bacteria.* Bacteria responsible for the second step of nitrification, the conversion of nitrite to nitrate. These microorganisms are produced by aerobic growth and decrease by endogenous respiration and decay. They are assumed to be present in the wastewater influent.
5. **X_S** [g COD m^{-3}]: *Slowly biodegradable particulate organic matter.* Fraction of the particulate organic matter COD which can be hydrolyzed and converted into readily biodegradable organic matter COD (S_S) and inert organic matter (S_I). A large fraction of X_S is assumed to originate from decay of microorganisms and it is also present in the wastewater influent.
6. **X_I** [g COD m^{-3}]: *Inert particulate organic matter.* It is the remainder after particulate organic matter hydrolysis and it increases by endogenous respiration of microorganisms. It is also present in the wastewater influent.

Note that particulate components are expressed in g COD m^{-3}, as it is common practice to express organic matter concentrations in all IWA models. Microalgae and bacteria biomass is transformed from COD to TSS (total suspended solids) assuming a ratio COD/TSS= 0.80 (Sperling, 2007; Khorsandi et al., 2014).

2.2.2. Dissolved components

7. **S_{NH4}** [g NH_4^+-N m^{-3}]: *Ammonium nitrogen*. Ammonium enters the ponds with the influent and is produced through endogenous respiration of all types of microorganisms in the model and decay of microorganisms. It is consumed through the growth of microalgae, heterotrophic bacteria (X_H) and during the first step of nitrification by ammonium oxidizing bacteria (X_{AOB}).
8. **S_{NH3}** [g NH_3-N m^{-3}]: *Ammonia nitrogen.* It is in acid-base equilibrium with ammonium (S_{NH4}), and comes into play in the model only as a gaseous compound. Its volatilization rate is modeled as a function of pH, temperature, and mixing intensity.
9. **S_{NO3}** [g NO_3^--N m^{-3}]: *Nitrate nitrogen.* Nitrate can enter the pond with the influent, although usually in negligible concentration. It is produced during nitrification by nitrite oxidizing bacteria (X_{NOB}). Nitrate can be assimilated by microalgae (X_{ALG}) and heterotrophic bacteria (X_H), and can also be used (consumed) as electron acceptor by heterotrophic bacteria, which are assumed to be facultative.
10. **S_{NO2}** [g NO_2-N m^{-3}]: *Nitrite nitrogen*. Nitrite can enter the pond with the influent, although usually in negligible concentration. It is generated as an intermediate step the nitrification process. It is consumed by nitrite oxidizing bacteria (X_{NOB}) and heterotrophic bacteria (X_H) during denitrification.

11. **S_{PO4}** [g PO_4^-- P m^{-3}]: *Phosphate phosphorus.* It enters with influent wastewater and is released from oxidation of organic matter. It is assimilated during the growth of microalgae, heterotrophic bacteria (X_H) and autotrophic bacteria (X_{AOB}, X_{NOB}). It is generated during respiration and decay of all microorganisms.
12. **S_{O2}** [g O_2 m^{-3}]: *Dissolved oxygen.* It is produced during photosynthetic growth of microalgae and it can be transferred to/from the atmosphere. It is consumed during aerobic respiration and decay of all types of microorganisms.
13. **S_{CO2}** [g CO_2-C m^{-3}]: *Dissolved carbon dioxide.* It is in chemical equilibrium with bicarbonate (S_{HCO3}) and carbonate (S_{CO3}). It is generated during respiration and decay, and can be transferred to/from the atmosphere. It is consumed by both microalgae (X_{ALG}) and autotrophic bacteria (X_{AOB} and X_{NOB}), and is produced during the growth of heterotrophic bacteria, and respiration and decay of all types of microorganisms.
14. **S_{HCO3}** [g HCO_3^--C m^{-3}]: *Bicarbonate.* It is in chemical equilibrium with carbon dioxide (S_{CO2}) and carbonate (S_{CO3}). It is consumed by microalgae.
15. **S_{CO3}** [g CO_3^{2-}-C m^{-3}]: *Carbonate*. It is in chemical equilibrium with bicarbonate (S_{HCO3}) and carbon dioxide (S_{CO2}). Carbonate cannot be directly used by microalgae and autotrophic bacteria.
16. **S_H** [g H^+ m^{-3}]: *Hydrogen ions.* They are involved in acid-base equilibria including the carbonate, ammonium, and phosphate systems. Hydrogen ions are produced by ammonium oxidizing bacteria (X_{AOB}) and heterotrophic bacteria (X_H). They decrease during the growth of microalgae and nitrifying bacteria (X_{NOB}), and during endogenous respiration and decay of all microorganisms.
17. **S_{OH}** [g OH^--H m^{-3}]: *Hydroxide ions*. They are in equilibrium with hydrogen ions.
18. **Ss** [g COD m^{-3}]: *Readily biodegradable soluble organic matter*. Fraction of the soluble organic matter directly available for biodegradation by heterotrophic bacteria (X_H). It is contained in the influent wastewater and is produced during the hydrolysis of biodegradable particulate organic matter (X_S).
19. **S_I** [g COD m^{-3}]: *Inert soluble organic matter*. Fraction of the soluble organic matter that is not readily available for biodegradation by heterotrophic bacteria (X_H). It is in the influent wastewater and is produced during the hydrolysis of biodegradable particulate organic matter (X_S).

2.3. Model processes

In this section, a detailed description of bacterial processes involved in wastewater treatment is described. A description of the microalgae processes, chemical equilibrium reactions, and transfer of gases to the atmosphere was reported previously (Solimeno et al., 2015).

Using Monod kinetics, bacterial processes were modelled in the same way as microalgae processes. The main inspiration for building the bacteria processes was the River Water Quality Model 1 (RWQM1) and Activated Sludge Model 3 (ASM3) (Reichert et al., 2001, Iacopozzi et al., 2007). A certain number of simplifications were

made in order to make easier the control of biochemical processes. This means that in comparison to ASM3, the model does not consider processes related to the storage of readily biodegradable soluble organic matter (S_S). Anaerobic biological processes, such as fermentation and sulfate reduction, which can sometimes be important in wastewater treatment, were also omitted because the relatively oxidized nature of microalgal-bacterial processes. Moreover, absorption and desorption of phosphate on particular matter were neglected.

Table S1 in the Supporting Information shows a list of the processes included in the complete model (bacteria and microalgae) and the equations describing their rates. Table S2 in SI shows the matrix of stoichiometric parameters. A complete list of parameters and stoichiometric coefficients used in the model is located in SI, Tables S3-S6.

- *Aerobic and anoxic growth of heterotrophic bacteria (X_H)* (Processes 4a, 4b, 5 and 6 in Table S1, SI). Growth of heterotrophic bacteria was modeled with Monod kinetics. Anoxic and aerobic heterotrophic processes use the same parameter and coefficient values. Anoxic processes include an additional reduction factor (η_H), similar to the ASM3 model (Gujer et al., 1999).

In aerobic conditions, heterotrophic bacteria assimilate the readily biodegradable substrate (S_S) (coming with the influent or produced during the hydrolysis of biodegradable particulate organic matter (X_S)), and growth consuming both ammonium and ammonia (S_{NH4}, S_{NH3}) and nitrate (S_{NO3}) as nitrogen source. Note that in the matrix of stoichiometric parameters (Table S2, SI) only the ammonium reaction rate is affected by bacterial growth because the concentration of ammonia is already in chemical equilibrium with it. Aerobic processes are generally the most responsible for the production of new bacteria biomass (Henze et al., 1987).

At dissolved oxygen concentrations less than 0.5 g m^{-3} heterotrophic bacteria use nitrate (S_{NO3}) as electron acceptor and convert it in nitrogen gas (N_2) (denitrification) (Korner and Zumft, 1986). The denitrification is implemented in the model as separating processes with S_{NO3} and S_{NO2} as substrates for heterotrophic bacteria (processes 5 and 6 in Table S1, SI), (Iacopozzi et al., 2007). In HRAP this process can occur at night, when photosynthesis is not happening (García et al., 2000)

The temperature dependence of bacterial processes is modeled with an Arrhenius type thermal factor ($f_{T,MB}$) (Sah et al., 2011; Langergraber et al., 2009; Reichert et al., 2001). This factor increases exponentially with temperature (T, given in °C) (Reichert at al., 2001):

$$f_{T,MB}(T) = \theta^{T-Topt} \quad (1)$$

where T_{opt} was assumed equal to 20 °C, and θ is the temperature coefficient, which was assumed equal for both heterotrophic and autotrophic bacteria.

- *Aerobic and anoxic endogenous respiration of heterotrophic bacteria (X_H)* (Processes 7 and 8 in Table S1, SI). These processes are modeled as the product between the

maximum rate of endogenous respiration ($k_{resp,H}$), the concentration of heterotrophic bacteria, the thermal factor (the same as used for growth), and the Monod function as it relates limiting oxygen and nitrogen concentrations respectively for aerobic and anoxic conditions. Endogenous respiration produces CO_2 and transforms alive biomass into inert organic matter (X_I).

- *Decay of heterotrophic bacteria (X_H)* (Process 9 in Table S1, SI). Decay of bacteria transforms alive biomass into dead slowly biodegradable (X_S) and inert (X_I) organic matter (Van Loosdrecht and Henze, 1999). This process is expressed as the product of the maximum rate of decay ($k_{decay,H}$) by the concentration of bacteria and the thermal factor (the same for growth). The process is assumed to continue with the same rate under aerobic and anoxic conditions (Henze et al., 1987).

- *Growth of autotrophic bacteria (X_{AOB} and X_{NOB})* (Processes 10 and 11 in Table S1, SI). These bacteria are responsible for the biological conversion of ammonium to nitrate nitrogen (nitrification) using molecular oxygen as electron acceptor. Nitrification is implemented in a two-step process (Iacopozzi et al., 2007).

- *Endogenous respiration of autotrophic bacteria (X_{AOB} and X_{NOB})* (Processes 12 and 13 in Table S1, SI). This process is modeled in the same way as the aerobic endogenous respiration of heterotrophic bacteria.

- *Decay of autotrophic bacteria (X_{AOB} and X_{NOB})* (Process 14 in Table S1, SI). This process is modeled in the same way as the decay of heterotrophic bacteria using different decay rates, $k_{decay,AOB}$ and $k_{decay,NOB}$, respectively for X_{AOB} and X_{NOB}.

- *Hydrolysis* (Process 15 in Table S1, SI). Hydrolysis is the process of transformation of slowly biodegradable particulate organic matter (X_S) into readily biodegradable soluble organic matter (S_S) catalyzed by heterotrophic bacteria.

2.4. Stoichiometric and parameter values

The complete stoichiometric matrix is presented in Table S2 in the Supporting Information and is based on the structure of IWA models (Petersen matrix). Values of physical, chemical and biokinetic parameters are shown in Table S3, SI. Mathematical expressions of the stoichiometric coefficients for each process are shown in Tables S5-S6, SI. Using Tables (S1-S2, SI), the reaction rate for each component of the model (r_i) is obtained using:

$$r_i = \sum_j v_{j,i} \cdot \rho_j \quad (2)$$

where i is the number of the component and j is the number of the processes; ρ_j is the reaction rate for each process j and $v_{i,j}$ is the stoichiometric coefficient. As

example, the reaction rate of heterotrophic bacteria (X_H) is described in the Supporting Information, page S13.

The expressions of stoichiometric coefficients related to microalgae and bacteria processes are based on the fractions of carbon hydrogen, oxygen, nitrogen and phosphorus (Table S6, SI).

3. Pilot plant and experimental verification

High quality experimental data for model calibration and validation were collected from three sets of triplicate HRAPs ponds (3.5 m^2 and 0.3 m deep), named South, Middle, and North, which were fed municipal wastewaters (Fig. 2). These small pilot raceways were located at a full-scale facultative pond-HRAP facility treating an average of 2,300 m^3d^{-1} of wastewater from the inland community of Delhi, California (Fig. 3). Data for this work were obtained during experiments conducted to optimize wastewater treatment in conjunction with algae biomass production, harvesting, and conversion to liquid biofuel.

Experimental data from the Middle pilot ponds were used. These ponds had 4.2-day hydraulic retention time (HRT), were fed with facultative pond effluent and were mechanically aerated at night from 6:00 pm to 6:00 am. Mechanical aeration was applied in order to maintain enough dissolved oxygen (DO) in the ponds at night when oxygen was not produced by photosynthesis in order to have nitrification activity. INDICA LA CANTIDAD DE BOMBAS DE AIRE, SU MARCA Y EL CAUDA DE AIREThe ponds received regular influent pulses (approximately 26.5 L/pulse) during the hours of 7:00 am to 4:00 pm. Each pond had a rotating paddle wheel with a rotation speed of approximately 10 rpm. In order to monitor the hourly DO, pH, and temperature (˚C), probes were installed per pond set. The probes recorded measurements using Neptune System's Apex Fusion software program.

Samples from influent and pond effluents were taken at 9:00 am ±2 hours for four to six consecutive days in June and July of 2016. Within 48 hours of sampling, assays were conducted to determine the concentration of ammonia (g N m^{-3}), nitrite (g N m^{-3}), nitrate (g N m^{-3}), total nitrogen (g N m^{-3}), alkalinity (g CaCO3 m^{-3}) and total suspended solids (g TSS m^{-3}). COD (g O_2 m^{-3}) influent was analysed only from the first sample of each experiment. These concentrations, as well as the hourly data from the Neptune software probes, were the main data for the model. Additionally, microscopic algal analyses were conducted on one of the four to six consecutive days for each experiment to identify the biological make-up within the ecosystem of each pond. Genera of microalgae common to the pilot ponds included *Chlorella*, *Closterium*, *Chlorococcum*, *Oscillatoria*, *Spirogyra*, *Synedra*, *Ulothrix*, *Westella*, *Coelastrum*, *Micratinium*, *Cyclotella*, *Nitzchia*, *Pediastrum*, *Scenedesmus*, and *Stigeoclonium*.

Samples were analysed according to Standard Methods (APHA 1995). Modifications were made to the methods for nitrate and total nitrogen according to Hach Company Methods 10206 and 10071 (Hach, 1992), respectively. Nitrite, nitrate,

and total nitrogen analysis were conducted using a Hach DR 3800 spectrophotometer (Hach, Loveland, Colorado) instrument. Ammonia analysis was conducted using a Timberline Model TL-2800 Ammonia/Nitrate Analyzer (Timberline Instruments, Boulder, Colorado) instrument.

4. The BIO_ALGAE model

The model was implemented in COMSOL Multiphysics^{TM} v5.1 software. The pilot raceways were represented in a 1D domain and were considered to be in a state of perfect mixing – a reasonably simplification due to their small size that streamlines the simulations to reduce computational time. The domain was 3.5 m long and a periodic condition was applied at boundaries to reproduce the continuous culture flow. Hydraulic and transport equations of aqueous phase species (i.e. dissolved and particulate) were added to represent the motion of the culture through the pond. Injection of dissolved oxygen (60 L/min) at night from 6:00 pm to 6:00 am was implemented in the model to reproduce the mechanical aeration of the middle ponds. Furthermore, assuming that each point of a section receives the same quantity of photons due to perfectly homogeneous of the pond, it was possible to calculate the light attenuation trough an average light intensity representing any point of the culture medium. In this way though the pond depth was not incorporated into the domain design (1D), the exponential decrease of light intensity as it penetrates into the pond has been considered. Average light intensity (I_{av}. [μmol $m^{-2}s^{-1}$]) was described using Lamber-Beer's Law and is attenuated by the presence of particulate components ($X_C = X_{ALG}+X_H+X_I+X_S+X_{AOB}+X_{NOB}$) and the depth (d) of the pilot raceways (Eq. 3).

$$I_{av} = \frac{Io \cdot (1-\exp(Ki \cdot X_C \cdot d)}{Ki \cdot X_C \cdot d} \quad (3)$$

where, I_o [μmol $m^{-2}s^{-1}$] is the incident light intensity and K_i is the extinction coefficient for particulate biomass [0.07 m^2 g^{-1}] (Molina et al., 1994).

A detailed description of hydrodynamic, transport of species, light intensity and the equations used in the model are reported in our previously work (Solimeno et al., 2016 and in Supporting Information, Tables S3-S4.

The model was calibrated using data collected during June 27, 2016 to June 30, 2016, from the first two Middle ponds (M1 and M2) in the triplicate set. Data from the third pond (M3) was not used due to lack of DO data.

Influent pond concentrations were used to run simulations. Average influent concentrations are shown in Table 1. Fractions of influent COD were estimated using values recommended by Henze et al., (2000). Accordingly, the proportion of each fraction was defined as: 22% S_S, 50% X_S, 10% S_I, 8% X_I, and 10% X_H. The initial concentrations of components in the Middle ponds M1 and M2 at the beginning of the

experiments, temperature and irradiance are shown in Table 2. Initial conditions from M1 pond were considered to run simulations. Unfortunately, the concentration of each particulate component in the pilot raceway at the beginning of the experiment was not known. Therefore, initial ratio of X_{ALG}, X_S, X_I, $X_{H,}$ X_{AOB} and X_{NOB} concentrations were quantified from initial TSS value (from M1 pond) based on previous experiments.

In this model 46 additional parameters were added to the 31 originally-implemented microalgae parameters (Solimeno et al., 2015), for a total of 87 parameters. Most of these parameters were obtained from the existing RWQM1 (Reichert et al., 2001), ASM1, and ASM3 (Gujer et al., 1999, Henze et al., 2000, Iacopozzi et al., 2007). Parameters related to temperature, photorespiration, carbon limitation and light attenuation were obtained from other literature cited in Supporting Information (S3).

Morris`s uncertainty method (Morris, 1991) was applied to screening which parameters had the greater influence on the simulation response. The detailed implementation of Morris's uncertainty method (Morris, 1991) is described in our previously work (Solimeno et al., 2016).

Based on previously uncertainty analysis, the model was calibrated by adjusting the values of maximum growth rate of microalgae (μ_{ALG}), the maximum growth rate and the decay of heterotrophic bacteria (μ_H and $k_{death,H}$) and the parameters related to the transfer of gases to the atmosphere ($K_{a,O2}$, $K_{a,CO2}$ and $K_{a,NH3}$). Calibration was performed comparing real data with simulation curves. Manual trial of parameters was used to match measured data as much as possible using graphical representations. Moreover, characteristic parameters ($\mu_{ALG,}$ $\mu_{H,}$ $k_{death,H,}$ $K_{a,O2}$, $K_{a,CO2}$ and $K_{a,NH3}$), values were adjusted in order to minimize the root mean square error (RMSE) between experimental data and simulated curves. After calibration the model was validated using data collected from July 17 to July 20, 2016 from the two Middle ponds M1 and M2.

Phosphorus was not considered in the simulations presented here since usually does not cause any growth limiting effect in high rate algal ponds treating wastewaters (Shilton, 2005, García et al., 2004).

Practical study cases were conducted to evaluate the relative effect of nutrients availability (i.e. nitrogen and carbon), temperature and light attenuation on microalgae growth. Moreover, total biomass production and the relative proportion of microalgae and bacteria as a function of different influent concentrations of organic matter were investigated. Keeping the same nutrient concentrations of the influent wastewater in the pond used for the calibration of the model and the same concentration of microalgae at beginning of the experiment, two scenarios were evaluated reducing COD influent and the initial concentration of bacteria (X_H, X_{AOB} and X_{NOB}), inert organic matter (X_I) and soluble organic matter (X_S) of 50% and 70%.

5. Results and discussion

5.1. Model calibration

The model was calibrated using duplicate experimental data of pH, DO, TSS, alkalinity, and nitrogen species concentrations from Delhi, California's pilot raceway ponds. The initial concentrations of components at the beginning of the experiments and the maximum and minimum water temperature and irradiance recorded for the four days of experiment, are shown in Table 2.TENDRIAS QUE DECIR QUE SE USARON LAS MEDIAS PARA LAS SIMULACIONES, NO? From the 87 parameters included in the BIO_ALGAE model (SI, S3), a sensitivity analysis of the maximum growth rate of microalgae (μ_{ALG}), the maximum growth rate and the inactivation of heterotrophic bacteria (μ_H and $k_{death,H}$) was performed to evaluate the impact of these parameters on simulation response. In this work, the sensitivity analysis of $K_{a,O2}$, $K_{a,CO2}$ and $K_{a,NH3}$ was neglected since the model results, from our previously works (Solimeno et al., 2016, 2015), have proven to be very sensitive to mass transfer coefficients to the atmosphere and therefore likely to be changed during the calibration. Note that the $\mu_{ALG,}$ μ_H and $k_{death,H}$ were selected because a global sensitivity analysis of whole set of model parameters (87) is quite unattainable objective unless high-end computational facilities are available. Moreover, these three parameters have demonstrated to influence mostly the model response during the calibration. Results of the sensitivity analysis, as reported in Figure S1 in the Supporting Information, have confirmed that these parameters selected ($\mu_{ALG,}$ μ_H and $k_{death,H}$) have the greatest impact on simulation outputs, therefore need to be calibrated. Once the most sensitive parameters of the model were identified, the calibration was performed in order to fit the model with the experimental data.

Table 3 presents the values of the six calibrated parameters which were used to obtain the results shown in Figures 4 to 6.

Fig. 4 shows the wave-like pattern of pH and DO concentrations in both the simulated and experimental data, which is consistent with known pond microalgae and bacteria activity. During night DO was not near 0 due to mechanical aeration. The model was able to match pretty well pH and DO values, in fact the the root mean square error of the simulation was low in relation to measured values ($RMSE_{pH}$= 0.11 and $RMSE_{DO}$= 0.62 g O_2 m^{-3}). This meant a good agreement between experimental data and simulations (Willmott et al., 1985; Bennet et al., 2013).

Fig. 5 shows the changes in both experimental and simulated bicarbonate (C_HCO_3), ammonium nitrogen (N_NH_4), nitrate (N_NO_3) and nitrite (N_NO_2) concentrations in the HRAPs. Bicarbonate and nitrate had relatively constant values in the different days, and the model was able to reproduce quite well the pattern of these experimental data. Ammonium and nitrite had clearly lower concentration than nitrate and much more relative variation. The RMSE values were 1.26 g C_HCO_3 m^{-3}, 0.73 g N_NH_4 m^{-3}, 1.72 g N_NO_3 m^{-3}, 0.16 g N_NO_2 m^{-3}. Altogether these results are indicative of a great nitrification activity, and it is very interesting to see how the model is very sensitive and can show slight diurnal variations which are not detected with the experimental samples. For example, it can be seen that higher simulated ammonia concentrations are observed at night when microalgae do not grow and DO concentrations are the lowest.

Average total biomass concentration in M1 and M2 changed from approximately 300 g TSS m^{-3} at the beginning of the experiment to 363 g TSS m^{-3} within four days. Simulated TSS concentrations (Fig. 6) match such growth patterns with a good accuracy ($RMSE_{TSS}$= 8.11 g TSS m^{-3}). Moreover, the Fig. 6 shows the simulated curve of microalgal (X_{ALG}) and bacterial biomass (X_H, X_{AOB} and X_{NOB}). As can be seen much of the biomass corresponds to microalgae (36.5% in average of TSS) and heterotrophic bacteria (28%). Nitrifiers biomass is comparatively very low (0.2%), however their activity is very important. The remaining solids are attributable to X_S (5%) and X_I (30.3%). This low amount of nitrifiers in comparison to other bacteria groups has been also obtained in previous simulation studies (Samsó and García, 2013; Krasnits et al., 2009; Silyn-Roberts and Lewis, 2001).

5.2. Model validation

The model was validated with experimental data obtained over four days. Solar radiation, temperature, and initial conditions of culture medium were different in the calibration and validation data sets (Table 2). Validation was conducted using the previous calibrated parameter values (Table 3).

Experimental results of the validation were similar to those of the calibration, and simulations matched pretty well the data. Fig. 7 shows the pH and DO fluctuations. The global error of the simulations was slightly higher than in the calibration ($RMSE_{pH}$= 0.38 and $RMSE_{DO}$= 1.88 g O_2 m^{-3}), but also the range of variation of the two parameters was much higher. Nitrates were again the N species with the higher concentration (Fig. 8). The RMSE values of each component were: $RMSE_{HCO3}$= 2.25 g C_HCO3 m^{-3}, $RMSE_{NH4}$= 0.85 g N_NH_4 m^{-3}, $RMSE_{NO3}$= 4.80 g N_NO_3 m^{-3}, $RMSE_{NO2}$= 0.18 g N_NO_2 m^{-3}. Simulated ammonium curve shows that the model was able to reproduce a wavelike trend of ammonium observed during the calibration, although with less accuracy ($RMSE_{NH4}$ values of validation was 0.85 g N_NH_4 m^{-3} against 0.73 g N_NH_4 m^{-3} calculated from calibration result).

Simulated TSS concentrations fitted well the experimental data and the RMSE had a similar value to those obtained before during the calibration ($RMSE_{TSS}$= 7.93 g TSS m^{-3}). Likewise of calibration, the model could to estimate microalgal (X_{ALG}) and bacterial biomass (X_H, X_{AOB} and X_{NOB}) over the four days of simulation (Fig. 9). Again much of the average biomass corresponds to microalgae (36.2% in average of TSS) and heterotrophic bacteria (30% in average), while nitrifiers (0.22%) had a low concentration. The remaining solids were X_S (4.8 %) and X_I (28.7 %). The relative proportion of particulate components respect to TSS obtained from model validation matches pretty well to those provided from the calibration.

5.3. Model applications

5.3.1. Analysis of factors affecting microalgae growth

These results of high nitrate concentration (in average 41.2 g N_NO_3 m^{-3} from calibration results) in conjunction with the relatively low microalgae biomass (in average 128 g TSS $m^{-3}$from calibration results) suggest C limitation for the growth of microalgae (note that nitrifiers and microalgae compete for inorganic carbon). In fact the C:N average ratio in the culture medium was 1:2. In general it is considered that microalgae growing in wastewater systems such as HRAP, in which no external carbon dioxide is supplied, are usually carbon limited (Park and Craggs, 2011; García et al., 2010; Oswald, 1988; Buhr and Miller, 1983).

With a deep analysis of model outputs this hypothesis could be tested and it could be investigated which factor is more affecting microalgae concentration. Fig. 10 shows the changes of Monod-limited functions values for inorganic carbon, nitrate and ammonium, as well as the light factor $f_L(I)$ (Processes 1a, 1b, in Table S1 in Supporting Information). As can be seen, Monod functions had values near 1 and therefore microalgae were no limited by carbon or nitrogen, rejecting the hypothesis of carbon limitation. In fact, microalgae were strongly influenced by the light factor $f_L(I)$, that had values clearly lower than 1 and reduced growth from 40 to 60 %. This factor takes into account the effects of light intensity (e.g. photoinhibition, photolimitation and light attenuation) and is considered to be the main limiting factor in pure microalgae systems (Larsdotter, 2006 REVISA QUE ESTA REFERENCIA SEA ADECUADA PARA "PURE SYSTEMS"). Fig. 11 shows the changes in incident light intensity (I_0) and subsequent changes in pond average light intensity (I_{av}) (Eq. 3), which had a direct effect on the values of the light factor. The effect of the light factor $f_L(I)$ on microalgae growth can be detected in Fig. 6b, where the slope of the main pattern of the curve slightly changes from days 1-2 to 3-4.

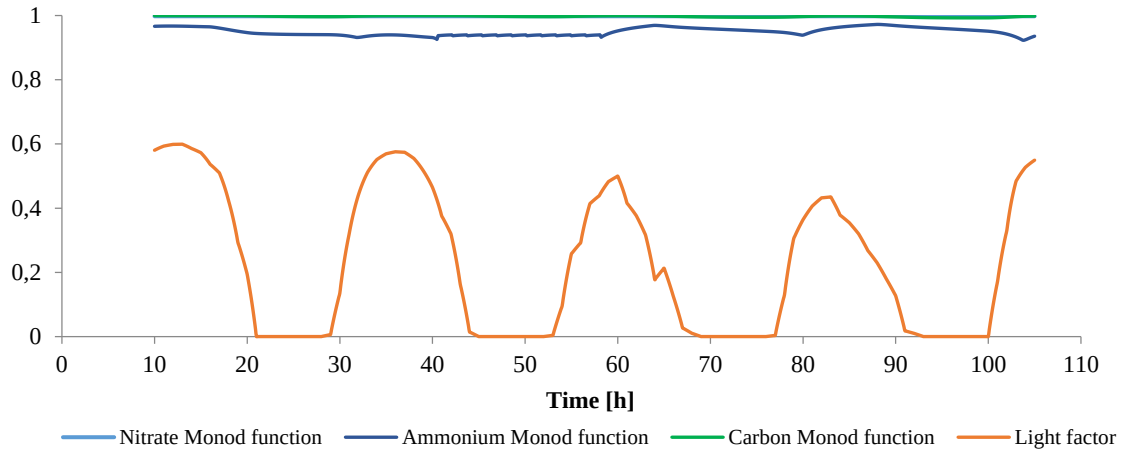

Fig. 10. Changes in the microalgae Monod-limited functions for inorganic carbon, nitrate and ammonium, and in the light factor (f_L) over the 4 days of the experiment. Results obtained from calibration.

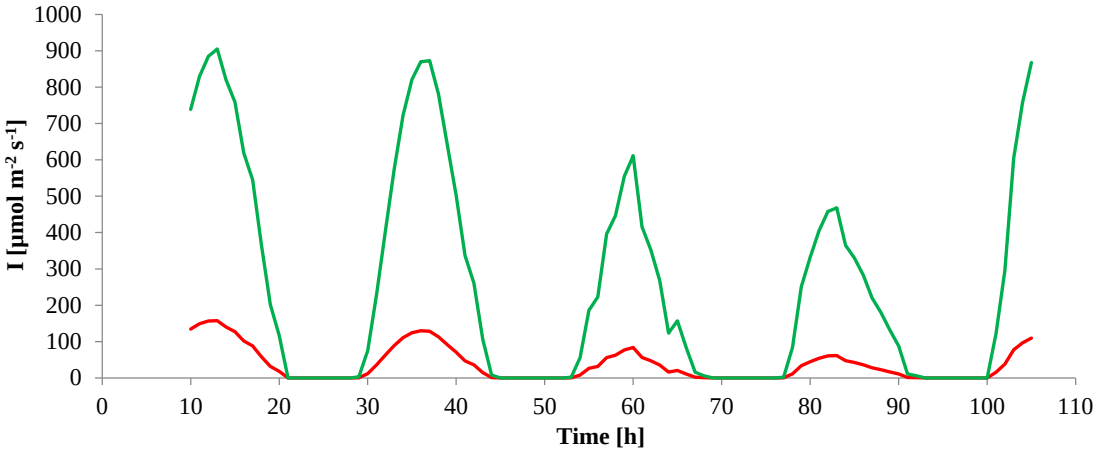

Fig. 11. Changes in in incident light intensity (I_0) (green line) and average light intensity in the pond (I_{av}) (red line) evolution over the 4 days of the experiment. Results obtained from calibration.

In addition, it is known that the growth of microalgae is highly dependent on temperature; it increase when optimum temperature is reached and drastically decrease when optimum temperature is exceeded (Solimeno et al., 2017; Dauta et al., 1990). The effect of the photosynthetic thermal factor on microalgae growth is shown in Fig. 12 (Processes 1a, 1b, in Table S1 in Supporting Information). As can be seen this factor lowered growth at night and midday (when water temperature was greater than 25 °C). However the global effect of the thermal factor was not as important as the light factor (having values ranging from 0.90 to 0.9.

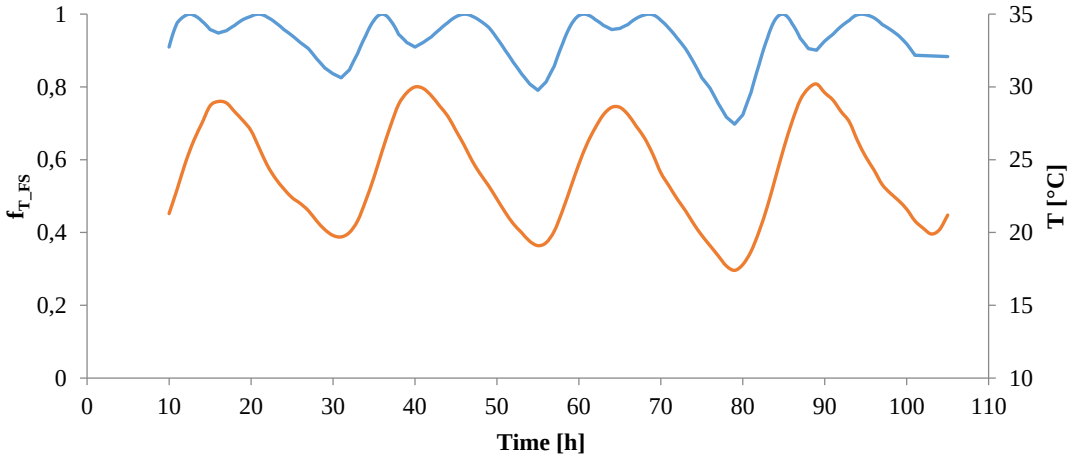

Fig. 12. Changes of the thermic photosynthetic factor (f_{T_FS}) (blue line) and the water temperature (T) (orange line) over the 4 days of the experiment. Results obteined from calibration.

5.3.2. Study case: effect of organic matter influent concentration on the relative proportion of microalgae and bacteria

According to the results presented in the previous section, attenuation of light within the pond was the main limiting factor on microalgae growth. Light attenuation

depends strongly on particulate components concentration; therefore it could be expected that with lower organic matter influent concentrations the relative proportion of microalgae could increase, due to a lower growth of heterotrophic bacteria. To test this hypothesis, results from calibration were compared with two scenarios where total COD influent and initial concentration used for the calibration of particulate organic matter (except microalgae concentration) were reduced by 50% and 70%, respectively. As can be observed in Fig. 13, simulations indicated that the total biomass production (in average of TSS) increased from 5.3 g TSS m^{-2} $d^{-1}$to 7.4 g TSS $m^{-2}d^{-1}$with the lower organic matter. Also the proportion of particulate components changed. Microalgae production is increased from 2.6 g TSS m^{-2} $d^{-1}$to 4.7 g TSS $m^{-2}d^{-1}$, while heterotrophic bacteria and inert particulate organic matter are decreased. The negative net production of slowly biodegradable particulate matter (X_S) is due to the conversion into readily biodegradable soluble organic matter (S_S) through hydrolysis process catalyzed by heterotrophic bacteria. A lower concentration of heterotrophic bacteria reduces the rate of hydrolysis. Autotrophy bacteria were not considered since their concentration is usually low.

Moreover, Fig. 13 shows the relative proportion of each particulate component respect to the total biomass. The proportion of microalgae in microalgae/bacteria biomass is increased trough an influent less loaded of particulate organic matter (from 56% to 77%). This result is in accordance with previous study by Park and Craggs, 2010, where the proportion of algae in the algae/bacteria biomass for an HRAP operating at 4-day hydraulic retention time (HRT) with CO_2 addition (approximately the same of our pilot raceways HRT= 4.4 d) was around 80.5%. On the other hand, microalgae production is relatively low (4.7 g TSS $m^{-2}d^{-1}$in average) comparing to values measured by Park and Craggs, 2010 (mean areal algal productivity = 16.7 ± 7.1 g $m^{-2}d^{-1}$). The low microalgae production suggests that microalgae are limited by carbon due to the absence of CO_2 addition. Fig. 14 shows that carbon Monod functions had values near 1 and therefore microalgae were no limited by carbon. Microalgae production is reduced due to the light attenuation by the high TSS concentrations in the culture medium. Although, the light factor (f_L) continues to reduce microalgae growth (~ 60%), an influent with less particulate organic matter slightly increases this factor promoting the growth of microalgae, especially at days 3-4, where the value of light factor (f_L) was most limiting (Fig. 14).

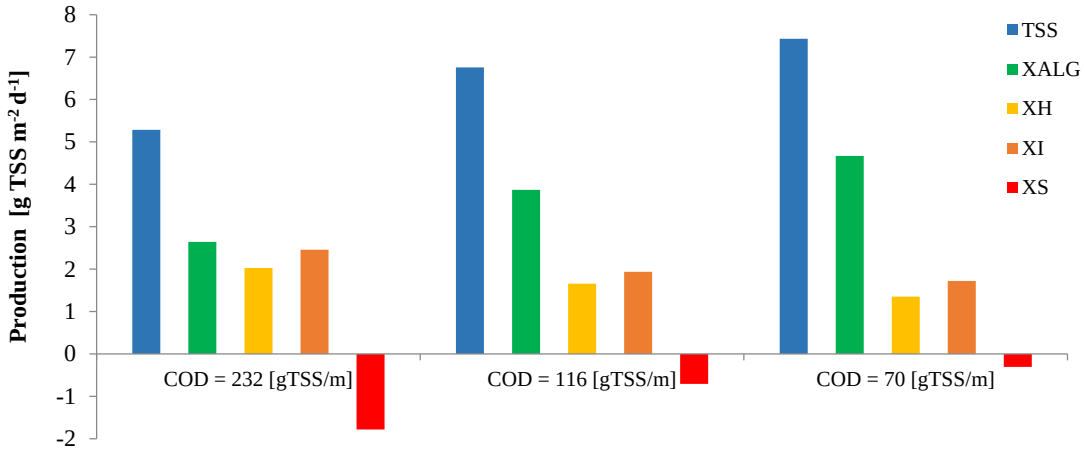

b)

Fig. 13. Comparison average biomass production (TSS) as function of COD influent. Proportion of particulate components (in average of TSS) as function of COD influent.

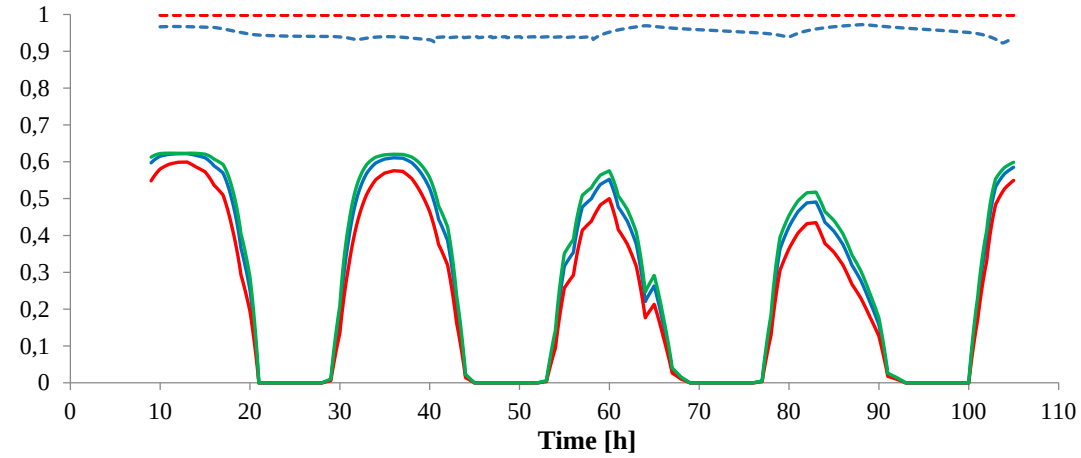

Fig. 14. Comparison between light factor (f_L) evolution and microalgae Monod-limited function for inorganic carbon over the 4 days of the experiment as function of COD influent. Red colour correspond to COD = 232 g TSS m^{-3}(calibration value) green to COD = 116 g TSS m^{-3} and blue to COD = 70 g TSS m^{-3}. Continues and dotted lines correspond to light factor and Monod function values, respectively.

6. Conclusion

In this paper the integral microalgae-bacteria model BIO_ALGAE for microalgae culture systems is presented. Biological processes, chemical and physical parameters affecting simultaneously microalgae and bacteria cultures were implemented in COMSOL Multiphysics™ software.

Based on RWQM1 and ASM3, BIO_ALGAE model considers carbon limitation on the growth of microalgae and autotrophic bacteria, and factors to represent photosynthesis, photolimitation, light attenuation, photorespiration, temperature dependency and the hydrodynamics of the system.

Uncertainty parameters from previously sensibility analysis were calibrated and validated by comparing simulated results and experimental data from triplicate pilot raceway ponds fed with facultative pond effluent for two different periods of four days. Results of the calibration and validation have indicated that the model was able to accurately reproduce total biomass concentrations, pH, dissolved oxygen and nutrient uptake.

The developed model has demonstrated to be a useful tool to simulate the performance of microalgae-bacteria wastewater treatment, in order to predict, for instance, the biomass growth of involved microorganisms (i.e. microalgae and bacteria) and their relative proportion as function of different COD influent. Moreover, the model could help to understand better physical and biochemical effects on the overall functioning system.

The next step in order to better understand microalgal-bacterial wastewater treatment would be to predict the production of microalgae and nutrient uptake using the model over a long period of time.

Acknowledgements

This research was supported by the Spanish Ministry of Economy and Competitiveness through the project DIPROBIO (CTM2012-37860). Alessandro Solimeno also acknowledges the FPU-AP2012-6062 scholarship provided by the Spanish Ministry of Education and Science. The construction and operation of the Delhi pilot facility and sample collection and analysis by California Polytechnic State University, San Luis Obispo, was the supported by the U.S. Department of Energy (Contract DE-EE0006317) with cost share from MicroBio Engineering Inc.

References

Abdel-Raouf, N., Al-Homaidan, A.A., Ibraheem, I.B. (2012) Microalgae and wastewater treatment. Saudi J.Biol Sci 19, 257-275.

APHA-AWWA-WPCF (2001). APHA-AWWA-WPCF Standard Methods for the Examination of Water and Wastewater (twentieth ed.)American Public Health Association, Washington DC.

Bennett, N.D., Croke, B.F.W., Guariso, G., Guillaume, J.H.A., Hamilton, S.H., Jakeman, A.J., Marsili-Libelli, S., Newham, L.T.H., Norton, J.P., Perrin, C., Pierce, S.A., Robson, B., Seppelt, R., Voinov, A.A., Fath, B.D., Andreassian, V., 2013. Characterising performance of environmental models. Environ. Model. Softw. 40, 1e20.

Bernard, O., Masci, P., Sciandra, A. (2009). A photobioreactor model in nitrogen limited conditions. In: Proceedings of the sixth conference on mathematical model- ling, Vienna.

Bitog, J.P., Lee, I.-B., Lee, C.-G., Kim, K.-S., Hwang, H.-S., Hong, S.-W., Seo, I.-H., Kwon, K.-S., Mostafa, E. (2011). Application of computational fluid dynamics for modelling and designing photobioreactors for microalgae production: A review. Computers and Electronics in Agriculture, 76(2), 131–147.

Bouterfas, R., Belkoura, M., Dauta, A., (2002). Light and temperature effects on the growth rate of three freshwater [2pt] algae isolated from a eutrophic lake. Hydrobiologia 489, 207-217.

Buhr, H.O., Miller, S.B. (1983). A dynamic model of the high-rate algal bacterial wastewater treatment pond. Water Res 17:29-37.

Christenson, L.B., Sims, R.C. (2012). Rotating algal biofilm reactor and spool harvester for wastewater treatment with biofuels by-products. Biotechnology and Bioengineering Volume 109, Issue 7, pages 1674–1684.

Dauta, A., Devaux, J., Piquemal, F., Boumnich, L. 1990. Growth rate of four freshwater algae in relation to light and temperatura. Hydrobiologia 207, 221-226

Diehl, J.M., Sciences, T.U.o.N.C.a.C.H.E., Engineering (2007). The Effect of Urea-ammonium-nitrate Fertilizer Amended with Urease and Nitrification Inhibitors on Nitrogen Cycling in Highly Organic Agricultural Soil. University of North Carolina at Chapel Hill.

Droop, M.R., (1968). Vitamin B2 and marine ecology. IV. The kinetics of uptake, growth and inhibition in Monochrysis lutheri'. J. Mar. Biol. Ass. U.K. 48, 689-733.

García, J., Green, B.F., Lundquist, T., Mujeriego, R. Hernández-Mariné, M., Oswald, W.J. 2006. Long term diurnal variations in contaminant removal in high rate ponds treating urban wastewater. Bioresource Technology 97: 1709–1715

García, J., Mujeriego, R., Bourrouet, A., Freixes, A. y Peñuelas, G. (2004). Operation and effluent quality of a small rural WWTP receiving sludge discharges from a WWTP of a slaughterhouse. Water SA 30, 197-202

García, J., Mujeriego, R. and Hernández-Mariné, M. (2000). High rate algal pond operating strate gies for urban wastewater nitrogen removal. Journal of Applied Phycology 12, 331-339.

Gehring, T., Silva, J. D., Kehl, O., Castilhos, A. B., Costa, R. H. R., Uhlenhut, F., Alex, J., Horn, H. and Wichern, M. (2010) Modelling waste stabilisation ponds with an extended version of ASM3, *Water Science and Technology*, 61(3), 713-720.

Gujer, W., Henze, M., Mino, T., and M. van Loosdrecht (1999). Activated Sludge Model No. 3. Water Science and Technology Vol 39 No 1 pp 183–193.

Hach Company. (1992). Hach water analysis handbook. Hach Company.

Halfhide, T., Dalrymple, O., Wilkie, A., Trimmer, J., Gillie, B., Udom, I., Zhang, Q., Ergas, S.J. (2015) Growth of an Indigenous Algal Consortium on Anaerobically Digested Municipal Sludge Centrate: Photobioreactor Performance and Modeling. BioEnergy Research 8, 249-258.

Henze, M., Grady Jr., C. P. L., Gujer, W., Marais, G. R., and Matsuo, T. (1987). Activated sludge model no. 1. Scientific and Technical Report No. 1, IAWPRC, London.

Henze, M., Gujer, W., Mino, T., van Loosdrecht, M. (2000) Activated sludge models ASM1, ASM2, ASM2d and ASM3.

Khorsandi, H., Alizadeh, R., Tosinejad, h., Porghaffar, H. 2014. Analysis of nitrogenous and algal oxygen demand in effluent from a system of aerated lagoons followed by polishing pond. Water Science & Technology 70.1 – 95.

Korner, H. and Zumft, W.G. (1986). Expression of denitrification enzymes in response to the dissolved oxygen level and respiratory substrate in continuous culture of Pseudomonas stutzeri. Appl Environ Microbiol. 1989 Jul;55(7):1670-6.

Krasnits E, Friedler E, Sabbah I, Beliavski M, Tarre S, Green M. Spatial distribution of major microbial groups in a well-established constructed wetland treating municipal wastewater. Ecological Engineering Volume 35, Issue 7, July 2009, Pages 1085–1089.

Iacopozzi, I., Innocenti, V., Marsili-Libelli, S., Giusti, E. (2007). A modified Activated Sludge Model No. 3 (ASM3) with two-step nitrification–denitrification. Environmental Modelling & Software 22, 847-861.

Langergraber, G., Rousseau, D., García, J., Mena, J., (2009). CWM1: a general model to describe biokinetic processes in subsurface flow constructed wetlands. Water science and technology : a journal of the International Association on Water Pollution Research 59(9), 1687–97.

Larsdotter, K. (2006). Wastewater treatment with microalgae-a literature review, Vatten 31–38.

Liang, Z., Liu, Y., Ge, F., Xu, Y., Tao, N., Peng, F., Wong, M. (2013) Efficiency assessment and pH effect in removing nitrogen and phosphorus by algae-bacteria combined system of Chlorella vulgaris and Bacillus licheniformis. Chemosphere 92, 1383-1389.

Milano, J., Ong, H. C., Masjuki, H.H. , Chong, W.T., Man Kee Lam, Ping Kwan Loh, Vellayan, V., (2016). Microalgae biofuels as an alternative to fossil fuel for power generation. Renewable and Sustainable Energy Reviews, Volume 58, May 2016, Pages 180-197.

Morris, M.D. (1991). Factorial Sampling Plans for Preliminary Computational Experiments. Technometrics, Vol. 33, No. 2. pp. 161-174.

Nurdogan, Y., Oswald, W.J. (1995). Enhanced nutrient removal in high rate ponds. Wat. Sci. Tech. 31: 33-44.

Oswald, W.J., 1988. Microalgal biotechnology. Borowitzka, M.A., Borowitzka, L.J (eds). Cambridge University Press.

Oswald, W.J., Gotaas, H.B. (1957). Photosynthesis in sewage treatment. Trans. Am. Soc. Civ. Eng. 122 73-105.

Oswald, W.J., Gotaas, H.B., Golouke, C.G., Kellen, W.R. (1957). Algae in waste treatment. Sewage Ind. Wastes 29 437-457.

Oswald, W.J., Golouke, C.G. (1960). Biological transformation of solar energy. Adv Appl Microbiol. 1960;2:223-62.

Park, J. B. K., Craggs, R. J. (2011a). Nutrient removal in wastewater treatment high rate algal ponds with carbon dioxide addition. Water Sci. Technol., 63(8), 1758-1764.

Park, J. B. K., Craggs, R. J. (2011b). Algal production in wastewater treatment high rate algal ponds for potential biofuel use. Water Sci. Technol., 63(10), 2403-2410.

Park, J. B. K., Craggs, R. J. (2010). Wastewater treatment and algal production in high rate algal ponds with carbon dioxide addition. Water Sci. Technol., 61.3 633-639.

Reichert, P., Borchardt, D., Henze, M., Rauch, W., Shanahan, P., Somlyódy, L., Vanrolleghem, P., (2001). River Water Quality Model no. 1 (RWQM1): II. Biochemical process equations. Water science and technology : a journal of the International Association on Water Pollution Research 43(5), 11–30.

Sah, L., Rousseau, D., Hooijmans, C.M., Lens, P., (2011). 3D model for a secondary facultative pond. Ecological Modelling 222(9), 1592–1603.

Samsó R., García J. Bacteria distribution and dynamics in constructed wetlands based on modelling results. Science of The Total Environment Volumes 461–462, 1 September 2013, Pages 430–440.

Sayeda, M. Abdoa, S.A. Abo El-Eninb, K.M. El-Khatibb, , , M.I. El-Galadb, S.Z. Wahbaa, G. El Diwanib, Gamila H. Alia. (2016). Preliminary economic assessment of biofuel production from microalgae. Renewable and Sustainable Energy Reviews Volume 55, pp.1147–1153

Serodes, J. B., Walsh, E., Goulet, O., De la Node, J. &Lescelleur, C. (1991). Tertiary treatment of municipal wastewater using bioflocculating microalgae. Can. J. Civ. Eng, 18, 940-944.

Shilton, A.N., Mara, D.D., 2005. CFD (computational fluid dynamics) modelling of baffles for optimizing tropical waste stabilization pond system. Water Science and Technology 51, 103–106.

Silyn-Roberts G, Lewis G. In situ analysis of Nitrosomonas spp. In wastewater treatment wetland biofilms. Water Res 2001;35:2731-9

Solimeno, A., Samsó, R., Uggetti, E., Sialve, B., Steyer, J.P., Gabarró, A., García, J. (2015). New mechanistic model to simulate microalgae growth. Algal Research 12, 350-358.

Solimeno. A., Samsó, R., García, J. (2016). Parameter sensitivity analysis of a mechanistic model to simulate microalgae growth. Algal Research 15, 217-223.

Solimeno. A., Acién, F.G., García, J. (2017). Mechanistic model for design, analysis, operation and control of microalgae cultures: Calibration and application to tubular photobioreactors. Algal Research 21, 236-246.

Sperling, M. V. 2007. Waste stabilization ponds. IWA Pubblishing, London, Uk.

Steen, P.v.d., Rahsilawati, K., Rada-Ariza, A.M., Lopez-Vazquez, C.M., Lens, P.N.L. (2015). A new photoactivated sludge system for nitrification by an algal-bacterial consortium in a photo-bioreactor with biomass recycle. Water Science & Technology, 443-450.

Suganya, T., Varman, M., Masjuki, H.H., Renganathan, S. (2016). Macroalgae and microalgae as a potential source for commercial applications along with biofuels production: A biorefinery approach. Renewable and Sustainable Energy Reviews Volume 55, March 2016, Pages 909–941.

Tricolici, O., Bumbaca, C., Postolacheb, C. (2014). Microalgae–Bacteria System for Biological Wastewater Treatment. Journal of Environmental Protection and Ecology 15, No 1, 268–276.

Van Loosdrecht M.C.M., Henze M. (1999). Maintenance, endogeneous respiration, lysis, decay and predation. Water Sci Technol 39:107-117.

Willmott, C.J., Ackleson, S.G., Davis, R.E., Feddema, J.J., Klink, K.M., Legates, D.R., O'Donnell, J., Rowe, C.M., 1985. Statistics for the evaluation and comparison of models. J. Geophys. Res. 90, 8995e9005.